

Spring 2024

Effectiveness of Aerial Monitoring of Spatial and Temporal Changes of Santa Catalina Island Rhodolith Beds

Charnelle Wickliff

Follow this and additional works at: https://digitalcommons.csumb.edu/caps_thes_all

This Master's Thesis (Open Access) is brought to you for free and open access by Digital Commons @ CSUMB. It has been accepted for inclusion in Capstone Projects and Master's Theses by an authorized administrator of Digital Commons @ CSUMB. For more information, please contact digitalcommons@csumb.edu.

**EFFECTIVENESS OF AERIAL MONITORING OF SPATIAL AND TEMPORAL
CHANGES OF SANTA CATALINA ISLAND RHODOLITH BEDS**

A Thesis

Presented to the

Faculty of the

Department of Marine Science

California State University Monterey Bay

In Partial Fulfillment

of the Requirements for the Degree

Master of Science

in

Marine Science

by

Charnelle Wickliff

Term Completed: Spring 2024

CALIFORNIA STATE UNIVERSITY MONTEREY BAY

The Undersigned Faculty Committee Approves the

Thesis of Charnelle Wickliff:

**EFFECTIVENESS OF AERIAL MONITORING OF SPATIAL AND TEMPORAL
CHANGES OF SANTA CATALINA ISLAND RHODOLITH BEDS**

DocuSigned by:



993886F78B544FC...

Alison Haupt, Chair

California State University, Monterey Bay

DocuSigned by:



12C12B4F71AF4A5...

Amanda Kahn,

Moss Landing Marine Laboratories, San Jose State University

DocuSigned by:



B1E71CC67799496...

Diana Steller,

Moss Landing Marine Laboratories, San Jose State University

DocuSigned by:



0D224745CD07438...

Corey Garza

University of Washington, Seattle

DocuSigned by:



E35BA879B9CD472...

Tom Connolly,

Moss Landing Marine Laboratories, San Jose State University



Cindy Juntunen (May 10, 2024 15:33 PDT)

Cindy Juntunen, Associate Provost of Research and Dean of Graduate Studies
Office of Graduate Studies & Research

Approval Date

Copyright © 2024

by

Charnelle Wickliff

All Rights Reserved

DEDICATION

To my parents, Oscar and Nolia Wickliff; and my grandparents, Alton and Ida Davis,
and Charlie and Lottie Wickliff

ABSTRACT

Effectiveness of Aerial Monitoring of Spatial and Temporal Changes
of Santa Catalina Island Rhodolith Beds

by

Charnelle Wickliff

Masters of Science in Marine Science

California State University Monterey Bay, 2024

The distribution and abundance of rhodolith beds off Santa Catalina Island, California are impacted by natural and anthropogenic factors. These complex, unattached coralline habitats provide food and shelter for important species; however, little is known about temporal variation in bed cover and distribution. Abiotic factors like heavy storms and surge can change bed boundaries and shape. Anthropogenic factors, such as disturbance from mooring chains, can create patchiness within beds. Studies of bed distribution and tracking changes in habitats have historically been done using labor-intensive SCUBA diving. This approach has excellent resolution at small scales but is limited in the temporal and spatial extent across which it can be employed. Emerging technologies, such as drones, may be able to address these limitations and provide an ability to survey large habitat areas beyond those which can be surveyed by SCUBA. Drones may also provide improved data resolution relative to satellite-based approaches to surveying coastal habitat. The objectives of this research were to 1) estimate the best conditions and methods for drones to assess live rhodolith beds, and 2) compare how well drone and diver surveys can be used to assess temporal and spatial shifts in rhodolith bed boundaries. Both drone and diver teams surveyed two beds—Isthmus Cove and Emerald Bay—at two times in different years. Drones best detected rhodolith beds when flying a lawnmower pattern overhead at 80 m altitude, with a 90-degree camera angle and 80% image overlap. Diver and drone survey methods provided significantly correlated estimates of rhodolith bed perimeter ($p=0.039$, $R^2=0.92$) and area ($p=0.004$, $R^2=0.993$), with a non-significant correlation in measuring live rhodolith cover ($p=0.533$, $R^2=0.218$) due to variability in diver data. These results suggest drone-derived estimates of rhodolith bed area and perimeter are comparable and complementary to subtidal SCUBA diver surveys. Drones can thus provide a long-term solution to conducting repeat subtidal surveys and will expand scientists' and resource managers' ability to monitor marine habitat over time.

Table Of Contents

ABSTRACT.....	v
Table Of Contents.....	vi
LIST OF TABLES.....	vii
LIST OF FIGURES.....	viii
ACKNOWLEDGEMENTS.....	x
CHAPTER	
Introduction.....	1
Methodology.....	4
Sites Description.....	4
Optimization of Drone Flights.....	6
Comparative Surveys of Two Rhodolith Beds.....	7
Data Analysis.....	8
Accuracy Matrix and kappa coefficient.....	9
Results.....	11
Optimization of Drone Flights and Image Classification.....	11
Comparison of Drone and Diver Surveys of Two Rhodolith Beds.....	12
Discussion.....	14
How this study compares with other remote sensing research.....	16
Drone limitations.....	17
Conclusions.....	18
References.....	20
Appendix I. Tables.....	27
Appendix II. Figures.....	35

LIST OF TABLES

Table 1. Drone Optimization Flights - record of each Catalina Island rhodolith bed flight by site (Isthmus and Emerald Bay) and date. Flights tested drone height (m), image overlap (%), camera angle (degrees), height, and image overlap. The presence indicates whether visible rhodolith beds were captured in orthomosaic (in part or whole).....	27
Table 2. Drone vs Diver comparison - accuracy Matrix and kappa coefficient for image classification at each site and year. The accuracy matrix calculates error on machine learning software that will determine how well an image is classified in 0 to 100% agreeance and the kappa coefficient measures how well the classification and ground truth align in -1 to 1 agreeance (St-Pierre and Gagnon 2020; Landis and Koch 1997; and Lillesand et al. 2014).	30
Table 3A - D. Perimeter (m) and area (m ²) estimates of rhodolith beds from SCUBA diver and drone surveys, and both is the overlap where sampling methods identified beds for two Santa Catalina Island rhodolith beds sampled at two time periods.	31
Table 4. Perimeter estimates and the comparison of the percent difference between diver and drone measurements over the two time periods at the two sites with drone and SCUBA diver measurements in meters (m). Percent difference was calculated as $[(\text{diver}-\text{drone})/\text{diver}]*100$. Negative values indicate when drone surveys generated larger perimeter measurements than diver surveys	32
Table 5. Area estimates and the percent difference between diver and drone estimates over two time periods at two rhodolith bed sites. Percent difference was calculated as $[(\text{diver}-\text{drone})/\text{diver}]*100$. Negative values indicate when drone surveys generated larger area measurements than diver surveys.	33
Table 6. Estimates of percent live cover calculations using SCUBA diver and drone survey data over two time periods in two rhodolith bed sites.....	34

LIST OF FIGURES

Figure 1. Map of known rhodolith beds around Santa Catalina Island based on historical diver surveys. Emerald Bay and Isthmus Cove, surveyed in this study, are in magenta. Image created in ArcGIS Pro. Rhodolith bed locations based on Tompkins and Steller (2016).	35
Figure 3. Orthomosaic partially constructed from a drone flight of the Emerald Bay rhodolith bed at Santa Catalina Island taken at a height of 100m, camera at 90%, 80% overlap on July 21, 2019. Glare and surface waves interfere with bed visibility.....	37
Figure 4. Orthomosaics of the Isthmus Cove rhodolith bed in January 2020 (A) and September 2021 (B). Yellow dots on the left part of the image denote the perimeter of a rhodolith bed as generated by diver-collected GPS points. On the right part of the image, an overlay depicts the area identified as rhodolith bed by diver survey only (yellow), drone survey only (blue), or detected by both (green).....	38
Figure 6. Relationship between diver and drone generated rhodolith bed perimeter measured at Isthmus Cove and Emerald Bay in 2020 and 2021 [$x=y$ line (red), simple linear regression $y=m(0.683)+106.579$ (blue), $p\text{-value}= 0.039$ and $R^2 =0.924$].	40
Figure 7. Relationship between diver and drone generated rhodolith bed area measurements for Isthmus Cove and Emerald Bay in 2020 and 2021 [1 to 1 line (red), simple linear regression $y=m(0.599)+902.530$ (blue), $p\text{-value}= 0.004$ and $R^2 =0.993$].	41
Figure 8. Side by side substrate classification images of Isthmus Cove (A, B) and Emerald Bay (C, D) rhodolith beds in 2020 (A, C) and 2021 (B, D). Left of image is the perimeter of the rhodolith bed estimated from diver-collected GPS points. On the right is the area of each rhodolith bed from the drone survey, where a maximum likelihood classification tool was used to depict dominant cover types: live rhodolith cover (pink), sand (yellow), other algae (green), and moorings and boats (white). Full extent of Emerald Bay is not depicted for 2020 and 2021 (C, D).	42
Figure 9. Relationship between diver and drone generated rhodolith bed live cover measurements for the two sites and two sampling dates [1 to 1 line (red), simple linear regression $y=m(3.115)+(-158.841)$ -blue, $p\text{-value}= 0.533$ and $R^2 =0.218$].	43

Figure 10. Overlay of drone (blue) and diver (pink) shapefiles from January 2020 sampling of the Emerald Bay rhodolith bed indicating that the drone captured more rhodolith habitat than divers could survey.	44
Figure 11. Overlay of drone (blue) and diver (pink) shapefiles from September 2021 sampling of the Emerald Bay rhodolith bed indicating that the drone captured more rhodolith habitat than diver could survey.	45
Figure 12. Evidence for drone use to identify boat mooring disturbance in rhodolith beds. Drone image of the Emerald Bay rhodolith bed showing boat mooring scars (blue triangle) and black and white 1m ² markers spaced 20m apart (orange arrow). Image from drone, 80m high, January 2020.	46

ACKNOWLEDGEMENTS

Thank you to Dr. Alison Haupt and Dr. Corey Garza for accepting me in your labs and providing me with the support and opportunities needed to shape and grow my graduate school experience.

Thank you to the rest of my committee members: Diana Steller, Amanda Kahn, and Tom Connolly for lending your expertise, flexibility, and feedback. Thank you to USC Wrigley Institute for Environmental Studies for having me as one of your fellows, your ample support, and for accommodating us. A special thank you to Taylor Eddy, Shelby Penn, Nina Mauney, Matt Edwards and his lab at SDSU, Kate Cauvanaugh and Kyle Cauvanaugh from UCLA, and so many others that made this possible. And last but not least, thank you to my family and friends for their love, support, and chocolate.

CHAPTER

Introduction

Foundation species are found globally on land and in the ocean and play an important role in the survival of many associated species (Bruno and Bertness 2001, Ellison et al. 2005, Thomsen et al. 2010, Angelini et al. 2011, Bulleri et al. 2016, Ellison 2019). Interactions between foundation species and other species are typically non-trophic, meaning that they are not a part of the food web (Ellison 2019). Some of the important roles of these structural habitat includes timber production (Angelini et al. 2011), serving as nursery grounds for fish and invertebrates (Boesch and Turner 1984, Carr 1989, Beck et al. 2001, Angelini et al. 2011), and shoreline stabilization (Orth et al. 2006, Koch et al. 2009, Angelini et al. 2011). With increasing natural and anthropogenic pressures, many foundation species and the habitats they provide are shifting, especially in marine and aquatic systems. Because of their ecological importance, foundation species are an important habitat to monitor.

A variety of methods exist for mapping and monitoring submersed habitats ranging from remote sensing methods (e.g., satellite, side-scan sonar), direct monitoring (i.e. SCUBA diving), and more recently, aerial drones; however, each method has benefits and limitations. Satellites have traditionally been used to study terrestrial systems but have been expanded to survey marine features such as monitoring kelp forest biomass (Bell et al. 2020) and fish stocks (Santos 2000). Satellite images are effective for looking at large-scale habitats (~1 km) but the resolution of most cost-effective or publicly available images is too coarse to detect fine-scale (<1 m) details within habitats. Satellite data are most useful for studying large-scale patterns where fine-scale temporal and spatial resolution are not necessary, because a satellite's spatial resolution may not be fine enough, or its orbit frequency may not match with the timescale needed for the

research (Johnston 2019). Side-scan sonar gives resolution 3m² or greater and has been used to map 50 m to 250 m sized submersed habitats (Oliver and Kvitek 1984, Degraer et al. 2008, Dondurur 2018). However, this method is equipment-intensive and relies on boats or ships, and is thus conducted episodically and relatively infrequently. SCUBA diving surveys are useful for observing and measuring patterns at small spatial scales in fine detail, but diving is labor intensive, generally covers small areas on scale of 10's of meters, and can be limited by diver bottom time of approximately one hour. (Ivošević et al. 2015). Aerial drones are newer technology that may be able to fill the gap between lower-resolution satellites and labor-intensive diving methods for mapping shallow habitats (Saccomanno et al. 2023) .

Drones can cover large areas on the scale of 50's of meters in approximately 45 minutes which is less time than diving and can give finer-scale resolution of habitats than satellite images (Ivošević et al. 2015). Drones equipped with a high-resolution camera with polarized lenses can capture the complexity and composition of various sized habitats to a few centimeters in resolution, filling in the time and scale limitations the other methods provide (Joyce et al. 2019, Garza, 2019). However, as aerial instruments drones may be limited for mapping submerged habitat when water clarity or light refraction affect their ability to resolve an image underwater. These factors can make it challenging to identify details on the seafloor (Joyce et al. 2019). To determine if drones are a useful tool for mapping submerged habitats, it is necessary to ground-truth surveys, assess weather conditions when surveys are possible and ideal, and optimize flight altitude and path type (Yang et al. 2020, St-Pierre and Gagnon 2020).

Rhodolith beds are an ideal habitat to test the efficacy of drones for surveying submerged habitats. Rhodolith beds are benthic ecosystems that are often visible in aerial surveys (Steller & Foster 1995), which increases the likelihood of detection via drones. Rhodolith beds are globally

distributed and support diverse benthic marine communities of invertebrates, fish, and other algae (Grall and Glemarec 1997; Steller et al. 2003, Nelson 2009). They provide habitats that support commercially harvested species at some locations such as scallops (Hall-Spencer et al. 1999), are nursery habitats (Kamenos 2004, Foster et al. 2013; Amado-Filho et al. 2012; Gabara et al. 2018) and serve as the foundation for diverse communities that include clams, pen shells, corals, crustaceans, echinoderms, molluscs, and polychaetes (Riosmena-Rodríguez 2015). They are important nursery grounds for many invertebrate species as well (Kamenos 2004, Foster et al. 2013; Amado-Filho et al. 2012; Gabara et al. 2018). Rhodoliths are red coralline algae that form spherical, non-attached, branching spheres that roll around on the seafloor, similar to tumbleweeds on land (Foster 2001). Multiple individual rhodoliths clustered together create a three-dimensional habitat called a rhodolith bed. Rhodoliths persist where light is sufficient for algal growth, and thus are mostly found in shallow waters (< 10m) (Foster 2001) although some have been found at depths of 270 m in tropical waters where light can penetrate (Littler and Littler 1984). With the increasing recognition of their ecological and economic value there is a need to better understand the spatial and temporal variability in their distribution.

Natural and anthropogenic disturbances can greatly affect rhodolith bed survival and morphology (Bosence 1976, Steller and Foster 1995). Beds typically occur in areas with moderate water motion, as motion is necessary for bed persistence by turning all individuals, which can reduce fouling, inhibit sediment accumulation, and stimulate growth (Bosence 1983; Steller & Foster 1995, Foster et al. 1997; Steller et al. 2009). However, water motion that is too rough can fragment rhodoliths or transport them to unfavorable habitats (Steller and Foster 1995, Bosence 1983). Heavy storms and surge can thus change the overall shape and location of beds and, combined with anthropogenic disturbances, can create areas with reduced cover or

patchiness (Steller et al. 2009, Tompkins & Steller 2016). Increasing coastal disturbance makes mapping existing rhodolith beds and following their distributions over time an important goal.

Numerous rhodolith beds exist near Santa Catalina Island, ranging in depth from 4 to 21 m with an average of ~10 m (Tompkins and Steller 2016). These beds support a diverse community of organisms, like invertebrates (Isopods, *Megastraea undosa*, and *Navanax inermis*) and macroalgae (Gabara et al. 2018). Easy access for divers and relatively clear waters makes Santa Catalina Island an ideal place to test the efficacy of drone surveys relative to established diver surveys. The objectives of this research were to 1) estimate the best conditions and methods for drones to assess live rhodolith beds, and 2) compare how well drone and diver surveys can be used to assess temporal and spatial shifts in rhodolith bed boundaries. I assessed the optimal conditions for drone flights and compared drone-generated measurements of bed perimeter, area, and live cover at Santa Catalina Island to those measured through SCUBA diver surveys. The assessment determines whether drones can be utilized as a survey method for rhodolith beds at Santa Catalina Island to expand scientists' and resource managers' ability to monitor beds over time.

Methodology

Sites Description

Shallow (<20 m) rhodolith beds are distributed around Santa Catalina Island, California in the lee of small bays (Figure 1, bed location based on Tompkins & Steller 2016). All beds are affected by seasonal sedimentation and waves, and by persistent anthropogenic disturbance of boat moorings. This year-round disturbance negatively affects the cover, distribution, and composition of rhodolith beds as the mooring chains bounce vertically on the sea floor with the rise and fall of swells and wind chop, and the vertical bouncing is exacerbated with an attached

boat (Tompkins, 2011). The motion results in a mooring scar when rhodoliths become fragmented in the wake of the crushing chain, creating areas of crushed rhodoliths (Serrano et al. 2016) and reduced community diversity and abundance (Tompkins and Steller 2016). These mooring scars may directly affect the overall cover of the rhodolith beds and potentially affect biodiversity of rhodolith bed ecosystems (Gabara et al. 2018). The shallow rhodolith beds at Santa Catalina Island are ideal locations to develop methods for remotely tracking bed dynamics over time using a drone, with paired SCUBA surveys to ground-truth the methods. This is primarily due to the relatively clear waters around the island and ease of diving access to them.

Rhodolith beds are found in protected bays along the north side of Santa Catalina Island (Figure 1) with an estimated collective depth ranging from 4.1 to 21m. The average area of all beds approximated 3,272 m² (as live rhodolith cover) in 2012 (Tompkins and Steller, 2016). To examine if a drone could detect submerged rhodolith beds, two shallow beds with well-defined edges were selected for surveys: Isthmus Cove and Emerald Bay (Figure 1). These beds have similar depth ranges (4.2 to 6.1 m from Tompkins 2011 survey) and are on the NW side of their respective coves. Lion Head Point provides protection for Isthmus and Indian Rock for the Emerald Bay bed (Tompkins 2016). All Santa Catalina Island beds, including these two, have supported consistently high live rhodolith cover during survey periods in 2011 (Tompkins & Steller 2016, Figure 1), 2013-2014 (Gabara et al. 2018) and from 2018-2020 (unpublished data, D. Steller & M. Edwards CA Sea Grant funding RHCE-04BTR). The overall perimeter, total bed area, and the percent cover of live rhodoliths within the bed area were assessed in this study.

Optimization of Drone Flights

To determine the best conditions to measure bed characteristics of perimeter (in meters), area (squared meters), and percent live cover, multiple flights were programmed using Pix4D software to generate multiple orthomosaics, and survey imagery was processed using Pix4D and Agisoft. Orthomosaics are generated when a series of pictures, containing GPS coordinates, are taken with an overlap in the aerial photograph and are reconstructed into an image of the landscape (Mills and McLeod 2013). To test for optimal drone flight conditions to visualize shallow Santa Catalina Island rhodolith beds, I conducted eight drone flights at each site: Isthmus on July 20, 2019 and Emerald Bay on July 21, 2019. Flights were conducted to evaluate the effects of image overlap, camera angle, and height on orthomosaic image quality. For flying over water, I flew the drone using the DJI Phantom 4 Pro V2 manufacturer recommended levels of image overlap (60%, 70%, and 80% overlap) at three different heights (60, 70, 80, and 100m) and followed the protocol by Joyce et al. (2019) of setting camera angle of 90° -nadir (directly pointed at the water), at different times in the day (morning and afternoon), and during different tide levels.

At low tide, the beds are covered with less water which will allow the drone to capture deeper parts of the bed than possible at high tide. In the morning, low-lying sun and calm winds reduce glare and wind stress on the sea surface, both of which can result in poor images producing a poor orthomosaic (Joyce et al. 2019; Mills and McLeod 2013). To verify that the drone could detect live rhodoliths, SCUBA divers placed two 1x1 m black and white site markers on rhodolith-covered benthos at each end of a 20 m transect within the living portion of the bed. In Pix4D , a grid was placed on a map over the hypothesized location of each rhodolith bed. The drone flew in a lawnmower fashion; georeferencing every image. Flight time ranged

between 7 to 10 minutes. Each flight was then uploaded and stitched into orthomosaics using Pix4D. Orthomosaics were used to measure the perimeter and area of the rhodolith bed, and percent cover of live rhodoliths (Figure 2).

Comparative Surveys of Two Rhodolith Beds

Based on results of the previous section, subsequent drone flights were conducted at 80 m altitude, with 80% image overlap, and 90% nadir camera angle to allow for maximum field of view. The flights for comparisons of drone and SCUBA surveys were conducted over the Isthmus and Emerald Bay rhodolith beds during two sampling time periods (January 12-13, 2020, and August 30- September 1, 2021). After uploading images to Pix4D cloud, Pix4D (and at times Agisoft Metashape, when Pix4D produced error) were again used to mosaic images into a single orthomosaic for each flight. Each orthomosaic was then imported into ArcGIS and a training sample manager was created by selecting random points of rhodoliths, sand, other algae, and boat/mooring buoys in the image. Maximum likelihood tool was used to classify the image for total cover of live rhodoliths within the beds, to measure the perimeter, and to measure the area. Bed area is defined as the area within the perimeter. Total cover of live rhodolith within a bed perimeter is defined as the area of living rhodoliths within the perimeter, minus scars and sand patches.

To evaluate the efficacy of drone surveys to accurately capture presence of living rhodolith beds, and to ground-truth drone imagery, SCUBA divers verified bed location, perimeter, and estimated percent live rhodolith cover for each site during each sampling period. To verify bed location, divers deployed two underwater site markers (1 x 1m² square made with 0.5 x 0.5 m² squares of alternating black and white) at the ends of a 20-m transect placed on the benthos within the live bed on an east-to-west heading. The marker captured in the drone images

provided visual confirmation. Divers determined the perimeter of the bed by swimming underwater, following the edges of the pigmented, live rhodolith material. At approximately 5-15m intervals along the bed edge, divers marked the bed edge by signaling with a surface buoy (tugging three times). A boat at the surface recorded GPS coordinates of each buoy location when divers gave the three-tug signal. Divers also collected depth data at each point from which they signaled. Finally, to estimate percent cover of living rhodoliths within the beds, divers estimated cover along three to four 20-m transects within each bed. At five fixed locations along each 20 m transect (at a distance of 0, 5, 10, 15, 20m), percent cover of substrate was estimated visually within 0.25 x 0.25 m² quadrats and photos were taken of each quadrat. Cover of the following substrate categories of primary substrate were visually estimated within each quadrat; live rhodolith, dead rhodolith, sand, and other along with secondary cover of macroalgae.

Data Analysis

Orthomosaics were classified into categories of live rhodolith, sand, other algae, and boats/mooring buoys using supervised maximum likelihood classification in ArcGIS 10.7.1 (Esri 2019). This method was preferred, because of the ability to use a training sample to aid in the classification of land use-type verse using the unsupervised object-based classification which segments an image into discrete objects before classifying each segment. The training sample created by selecting random points of rhodoliths, sand, other algae, and boat/mooring buoys in the image (training samples per classification: rhodolith (n=25), sand (n=15), other algae (n=20), boats and mooring (n=10); sample size was based on what was visible in the image). After creating and editing the training file with these four classes, I ran a classification tool for each training sample to assign each pixel to one of the three classes. The estimation from this tool was

used to compare live rhodolith cover from the live rhodolith cover estimate generated from the SCUBA diver data.

Accuracy Matrix and kappa coefficient

To calculate statistical accuracy of the classified orthomosaics, an accuracy matrix and kappa coefficient of agreement were created using ArcGIS and exported to Microsoft Excel (St-Pierre and Gagnon 2020). The accuracy matrix calculates error on machine learning software that will determine how well an image is classified, ranging from 0 to 100% agreement and the kappa coefficient measures how well the classification and the points selected for ground-truth align in one-to-one agreement (Landis and Koch 1997, Lillesand et al. 2014, St-Pierre and Gagnon 2020). A kappa coefficient of ≤ 0 indicates a very poor/meaningless classification and a value of 1 indicates a perfect classification (Landis and Koch 1997, Lillesand et al. 2014, St-Pierre and Gagnon 2020).

To compare perimeter and bed area estimates between drone and diver data, the union tool in ArcMap was used to generate a geometric union between multiple feature classes and layers (Esri 2019). The drone generated and diver generated shapefiles from each location were input into ArcMap for each time period, then the union tool was used to create an output of the two input shapes (drone-collected and diver-collected data) and a third shape where the two layers overlap. From these three images, the tabulate area tool was used to measure the live cover estimated by both survey types and areas where the two methods did (and did not) overlap in mapping the beds. Due to how the shapefiles of the two methods overlap, no information is lost in generating the data.

To calculate the percent difference in perimeter and area estimated by the two methods, I used the following equation to compare the percent difference between the two methods relative

to a one-to-one relationship. I subtracted the drone data (either perimeter or area) from the diver (standard) data and divided the value by the diver (standard) data, then multiplied by it by 100 using the following equation $[(\text{diver}-\text{drone})/\text{diver}] * 100$.

To test how well the diver-generated rhodolith parameters (perimeter, area, and live rhodolith percent cover) correlated with drone-generated parameters, I ran a simple linear regression (with a significance level $\alpha = 0.05$) and calculated an R² value. Diver-generated data were used as the observed data and the drone-generated data were used as the expected data to calculate the root mean square deviation (RMSD), which is the standard deviation of the residuals in the dataset or the mean of the residuals as they relate to the mean. The RMSD value gives the standard deviation of the residual from the model. A paired t-test was used to test for significant (p-value < 0.05) differences between drone and diver measurements for each site and time period. A p-value greater than 0.05 would indicate that the drone data and diver data did not significantly differ from each other. This test has low statistical power due to a small sample size and the statistical design of looking for “no difference” rather than a difference. Even if there was a large difference between methods, there is still a high probability that the test would not show a statistically significant difference.

For the drone-generated data, live rhodolith cover was calculated using the area of live rhodolith area identified using image classification within the total area of the bed, as seen in the orthomosaic. For diver-generated data the mean percent cover of live rhodolith cover was calculated from quadrat sampled cover data collected at each site for each sampling time. For each sampling date and site, each diver transect generates five live rhodolith cover estimates per transect for each site. The mean live rhodolith cover for each transect was calculated, and then

the mean of the means for each site was calculated to generate the live cover estimates from both sites and time periods.

Results

Optimization of Drone Flights and Image Classification

The drone was able to detect rhodolith beds at Isthmus Cove and Emerald Bay multiple times, but with mixed success. Many flights resulted in images of landscape or just the nearby rock formation (Figure 3). Each flight produced a different number of total images in the orthomosaic, however the number of non-stitched images was not available (Table 1). It is unclear why some orthomosaics were unable to stitch well while others produced high-quality images of rhodolith beds. It is also unclear why an orthomosaic would not produce an image at all resulting in an error. Errors and images without rhodoliths are most likely a result of mapping over a body of water as noted by the manufacturer. The reason why there is a high overlap in images is to reduce/account for these types of errors. The flight settings that had the most of the rhodolith beds presence are 80 m height, 90% camera angle, 80% camera overlap. Flights were ideally conducted in the morning (07:00 am - 09:30 am) and/or at low tide (0.0 ft to 3.0 ft) for optimal weather and ocean conditions to produce a clear image (Table 1A-D). Although no flights were canceled due to weather conditions, the September 2021 flights were flown during a small weather window because of increased wind and rain in the forecast.

The overall accuracy of the image classification average was 73.4% ($n = 4$, ± 18.1 SD) with average kappa coefficients 0.620 (Table 2). The accuracy of Isthmus Cove image classification for 2020 and 2021 were 68.9% and 56% with kappa coefficients of 0.53 and 0.41

respectively. The accuracy of Emerald Bay image classification for 2020 and 2021 were 98.9% and 70% with kappa coefficients of 0.98 and 0.55 respectively.

Drone surveys estimated a higher perimeter and bed area values for all times and sites sampled relative to diver-based estimates. For the Isthmus Cove rhodolith bed surveys, drone estimates of the bed perimeter were roughly 20m greater and bed area estimates were roughly 40m² greater relative to diver-based estimates (Figure 4A and Table 3A). Similarly, the Isthmus Cove 2021 rhodolith bed survey also showed drone estimates having a higher perimeter and area value (roughly 15 meters, 700m²; respectively) relative to diver estimates (Figure 4B and Table 3B).

For Emerald Bay 2020 surveys, perimeter measurements were larger (roughly 20 meters) with drones than divers; area measurements were also higher (roughly 1,400 m²) with drones (Figure 5C and Table 3C). Emerald Bay 2021 drone measurements for perimeter were higher (roughly 90 meters) than divers; area drone measurements were also higher than diver estimates (roughly 2,685 m²) (Figure 5D and Table 3D).

Comparison of Drone and Diver Surveys of Two Rhodolith Beds

Perimeter estimates were between +5.7% to -14.1% different between diver and drone surveys (Table 4). Negative values indicate when drone surveys generated larger perimeter measurements than diver surveys. This can be attributed to a larger perimeter shapefile in ArcMap being created without a diver GPS point to ensure the full rhodolith bed was captured. Perimeter estimates from diver and drone surveys were not significantly different (Paired t-test, $p = 0.32$, 95% confidence intervals = -76.4%, 36.4%). In addition, drone-derived perimeter estimates were significantly correlated with diver estimates, with some variation from the mean (linear regression in the residuals $y=m(0.683)+106.579$, $p = 0.039$, $R^2 = 0.924$, Figure 6) with

the RMSE being 36.617 meters (the mean of the residuals from the model line), indicating that the drone and diver perimeter measurements were correlated.

Percent differences in area ranged from -1.41% to -30.53% (Table 5), again indicating that drone measurements were greater than diver measurements. This can be attributed to drawing a larger perimeter as stated in the previous paragraph. The relationship between diver and drone measurements were not significantly different (Paired t-test, $p = 0.113$, 95% confidence intervals = -3022.7%, 538.4%). Also, when examining how well drone-derived estimates of area correlated with the same estimates for divers, there was again a significant correlation with some variation from the mean (linear regression in the residuals $y=m(0.599)+902.530$, $p\text{-value} = 0.004$, $R^2 = 0.993$, Figure 7) with the RMSE being 1575.48 m² (the mean of the residuals from the model line) indicating that the drone and diver area measurements were similar.

Live rhodolith cover from drone surveys ranged from 70.1% to 76.5% overall for both sites (Figure 8, Table 6). Live cover estimates from diver surveys were more variable, from 46.9% to 93.3% with Emerald Bay having the most live cover. Diver-generated and drone-generated rhodolith live cover measurements were not significantly different (Paired t-test, $p = 0.714$, 95% confidence intervals = -33.1%, 25.7%). When examining how well drone-derived live cover estimates correlated to diver live cover data, there was no significant correlation with some variation from the mean (linear regression in the residuals $y=m(3.115)+(-158.841)$, $p\text{-value} = 0.533$, $R^2 = 0.218$, Figure 9) with the RMSE being 16.417% (the mean of the residuals from the model line), indicating that the live cover measurement are highly variable using diver survey methods. Both sites exhibited a reduction in live cover of roughly 5% from 2020 to 2021.

Discussion

This study demonstrated that drones are an efficient tool for mapping submerged marine habitats. Drone estimates of total rhodolith area were on average higher than diver estimates of all rhodolith bed parameters, which indicates that drones may capture broader areas of the seafloor more efficiently than divers or that they overestimate at times. Drones were also not as precise as divers at detecting bed perimeter due to water visibility which can cause pixels of the image to not be as clear (Joyce et al. 2019). Drones may not be as capable at capturing detailed edges, or habitat boundaries as divers. Additionally, drone-generated estimates of area, perimeter and cover may have been higher out of caution of drone users wanting to fully encompass the rhodolith bed in the analytical process. Despite the higher estimates of bed perimeter, drone estimates were comparable to diver methods and can be used as a supplement for monitoring underwater rhodolith habitats. Drones are a cost-effective way to survey marine habitats (Eddy 2021, Cavanaugh et al. 2021). The ability to search for, locate, and map underwater beds with drones can save time and energy that would allow divers to focus on the habitat details that the drones cannot detect, like species diversity.

For mapping Santa Catalina Island rhodolith, the optimal settings for drone surveys were 95% image overlap flown 80 m above the water surface and in the time window of 7:00 am to 9:30 am. This set-up may not be the best settings for other habitats and locations, thus initial drone flight ground truthing is necessary for each study. For example, for giant kelp that grows along the waters' surface, drone flights with 75% image overlap and a height of 120 m were sufficient (Saccomanno et al. 2023) for mapping. Drone flights with 85% image overlap and heights of 114 m were sufficient to map seagrass beds on an island off of Portugal (Kellaris et al.

2018). Habitat, location, and flight testing will be determining factors in optimal drone flight methods for any given study.

While drone and diver surveys largely agreed, the discrepancy in drone versus diver measurement resulted from mapping the perimeter of Emerald Bay's rhodolith bed. While not statistically significant, the drone survey detected a much larger habitat than the diver could survey (Figure 10 and Figure 11). The divers did not detect a large area of habitat on the seafloor. The reason for this discrepancy could be due to a sandbar that may have blocked divers' view of more habitat, or from not being able to explore further into the bed because of time and air constraints. Emerald Bay has a denser cover of rhodolith in a certain location and is well protected by Indian Rock, a rocky reef (Tompkins 2016). The reef may contribute to the bed being denser. To compare between the two methods for this work, I measured the perimeter of the rhodolith bed at Emerald Bay to better compare with the diver surveys. However, the drone's ability to capture broader habitat opens the possibility for broader exploration of Emerald Bay's rhodolith beds. In other locations where drones are being utilized, more habitat is being detected than historical data collection methods had detected (Eddy 2021, Saccomanno et al. 2023). For example, drone surveys captured more *Nereocystis luetkeana* (bull kelp) blades than Landsat sensors due to their finer spatial resolution (<0.1 m) (Saccomanno et al. 2023). In the same study, the drones captured new habitats that could not be detected by historical methods. These assessments demonstrate a drone's usefulness as a survey method for marine habitats and expand scientists' and resource managers' ability to monitor beds over time.

Other caveats associated with these study results can be related to human errors in collecting GPS points and habitat selection when training the image classifier in ArcMap. A factor that may be responsible for differences in the drone and diver perimeter measurements is

the potential lag in buoy line the divers used to give the signal to the boat crew. This can be seen at a couple of locations in the shapefiles where the boat and dive team were making a counterclockwise turn around the bed perimeter and the buoy was further away from beds' edge. There may not be a way to correct this or accurately account for this type of error. However, due to the nature of ocean currents, the position of the buoy would never be directly over the divers. This error is something to be aware of but is not likely a big source of error because the currents would overestimate the perimeter at one edge and underestimate at the other canceling out the error.

How this study compares with other remote sensing research

Other research using remote sensing to map submerged habitats (e.g. kelp canopies and seagrass beds) has shown that aerial surveys are an effective way to monitor marine habitat distributions. Cavanaugh et al. (2021) found that drones were capable of measuring giant kelp *Macrocystis pyrifera* distribution from the sea surface, despite current or tides. They reported that timing of data collection was easier to set with a drone, because they could collect data quickly during a favorable time/weather window unlike satellite images. The mapping flights in this study conducted on Santa Catalina Island ranged from seven to nine minutes long and were executed during the optimal weather condition for each sampling period. For comparison, Ventura et al. (2016) used a drone and a towed camera to map coastal fish nursery grounds and found that drone images coupled with underwater surveillance provided useful information in the structure and characteristics of a seagrass bed of the Mediterranean Sea. Similarly, the data gathered through diver and drone surveys for this work, including the image classifications, are the beginning steps to fully characterize the rhodolith beds around the island. In contrast, Kellaris et al. (2019) compared drones with satellite and aircraft imagery with the expectation that the

higher resolution in drone image would be able to decipher seagrasses in a heterogeneous habitat. However, they found the drone surveys to be challenging to schedule and process due to the unpredictable weather as well as the inability to distinguish seagrass below 3 - 4 m depth due to heavy overcast. They concluded that drones could be used to map underwater habitats but cautioned that optimal weather conditions were important. For the work presented here, weather conditions played an important constraint on when I could fly. In the event of predicted high winds (>8 knots), I would postpone flights until the next day because higher wind speeds increase wind shear on the surface, making visually capturing the beds difficult (e.g. Figure 3). Monitoring for high wind conditions during drone imaging flights is important because resulting surface water movement can distort images and increase drone speed past the legal limit. Winds and foul weather in general are common factors affecting drone surveys and are avoided as much as possible (Kellaris et al. 2019, Cavanaugh et al. 2021).

A potential area for future research on the effectiveness of drones for mapping rhodolith bed disturbance would be on the prevalence and dynamics of boat mooring scars (Figure 12) on rhodolith bed health (Tompkins & Steller 2016). Another would be examining seasonal changes on rhodolith beds movement and if heavy storms affect overall bed dimensions given rhodolith's tendency to move around (Steller and Foster 1995). Given the motility of rhodoliths and the beds, drones can also be used to monitor changes on a smaller time-scale than seasonality and monthly monitoring would be easier to conduct with drones versus divers.

Drone limitations

An unforeseen limitation occurred in this study due to poor cellular service at Emerald Bay. As a result, I would preload the map the night before flying which made for an easier drone-remote connection. Due to poor on-site connection if the drone could not connect, remote

flying could not occur. A drone with Real Time Kinematic (RTK) can overcome this limitation, because they are connected to a Networked Transport of RTCM via Internet Protocol (NTRIP) which uses a networking system to make connections versus cellular service. Other considerations included wildlife encounters that can pose a potential hazard. On a preliminary trip to Santa Catalina Island in October 2019, on a beach near Emerald Bay's youth camp and after gaining permission to fly from the beach, a camp manager warned that there was a nest of meat bees on site. I quickly found myself surrounded by meat bees as they were swarming the kelp wrack. This poses no threat to the drone, but has potential to cause harm if the drone pilot is unable to remain calm in this type of stressful environment.

Conclusions

Drones can provide visual data that have recently proven useful for studying marine habitats. They are being used to monitor kelp canopy and rocky intertidal habitats, and now also rhodolith beds, along the coast of California (Garza 2019, Bell et al. 2020, St-Pierre et al. 2020; Cavanagh et al. 2021, Eddy 2021; Saccomanno et al. 2023). When the right criteria are met; clear waters, low tides, and low wind, drones are capable of mapping submerged habitats. This study demonstrated that drones can be used to map the size and condition (live cover) of live rhodolith beds and, in combination with diver surveys, can improve spatial and temporal resolution to monitoring efforts.

Until this study, research using drones to map rhodolith beds was limited and the results of this study will help future researchers. With the global distribution of rhodoliths and the rapidly increasing use of drones in marine science, this research can be expanded in various ways. It can aid surveys in a wide variety of habitats including shallow coral reefs and other benthic habitats in relatively clear water (Ventura et al. 2018, Kabiri et al. 2020). This study

suggests that drone use can be expanded to measure the effects of water movement on rhodolith bed distribution. By monitoring distribution easily, surveys can be conducted to determine where beds may be affected by natural disturbance of water movement and how the movement changes the perimeter of the bed over time (Frederiksen et al. 2004, Veettil et al. 2020). Drones can also be used to measure anthropogenic disturbances in rhodolith and seagrass beds such as mooring impacts and dredging (Erftemeijer and Lewis III 2006, Luff et al. 2019) and/or non-anthropogenic disturbances such as severe storms (Oprandi et al. 2020).

References

- Amado-Filho, G.M., Moura, R.L., Bastos, A.C., Salgado, L.T., Sumida, P.Y., Guth, A.Z., Francini-Filho, R.B., Pereira-Filho, G.H., Abrantes, D.P., Brasileiro, P.S. and Bahia, R.G., (2012). Rhodolith beds are major CaCO₃ bio-factories in the tropical South West Atlantic. *Public Library of Science One*, 7(4), 35171.
- Angelini, C., Altieri, A.H., Silliman, B.R., and Bertness, M.D. (2011). Interactions among foundation species and their consequences for community organization, biodiversity, and conservation. *BioScience* 61, 782–789.
- Beck, M. W., Heck, K. L., Able, K. W., Childers, D. L., Eggleston, D. B., Gillanders, B. M., Halpern, B., Hays, C.G., Hoshino, K., Minello, T.J., Orth, R.J., Sheridan, P.F., and Weinstein, M. P. (2001). The identification, conservation, and management of estuarine and marine nurseries for fish and invertebrates: a better understanding of the habitats that serve as nurseries for marine species and the factors that create site-specific variability in nursery quality will improve conservation and management of these areas. *Bioscience*, 51(8), 633-641.
- Bell, T. W., Allen, J. G., Cavanaugh, K. C., and Siegel, D. A. (2020). Three decades of variability in California's giant kelp forests from the Landsat satellites. *Remote Sensing of Environment*, 238, 110811.
- Boesch, D. F., and Turner, R. E. (1984). Dependence of fishery species on salt marshes: the role of food and refuge. *Estuaries*, 7, 460-468.
- Bosence, D.W.J. 1976. *Paleontology*, Vol.19 (2) 365-395, pls 52-53.
- Bosence, D. W. (1983). The occurrence and ecology of recent rhodoliths—a review. In Coated grains. *Springer*, 225-242).
- Bruno, J.F., and Bertness, M.D. (2001). Habitat modification and facilitation in benthic marine

- communities. *Marine Community Ecology*, (Sinauer Associates), 201–218.
- Bulleri, F., Bruno, J.F., Silliman, B.R., and Stachowicz, J.J. (2016). Facilitation and the niche: implications for coexistence range shifts and ecosystem functioning. *Functional Ecology*. 30, 70–78.
- Carr, M. H. (1989). Effects of macroalgal assemblages on the recruitment of temperate zone reef fishes. *Journal of Experimental Marine Biology and Ecology*, 126(1), 59-76.
- Cavanaugh, K.C., Cavanaugh, K.C., Bell, T.W., and Hockridge, E.G. (2021) An automated method for mapping giant kelp canopy dynamics from UAV. *Frontiers in Environmental Science*, 8, 587354. <https://doi.org/10.3389/fenvs.2020.587354>
- Degraer, S., Moerkerke, G., Rabaut, M., Van Hoey, G., Du Four, I., Vincx, M., Henriët, JP., and Van Lancker, V. (2008). Very-high resolution side-scan sonar mapping of biogenic reefs of the tube-worm *Lanice conchilega*. *Remote Sensing of Environment*, 112(8), 3323-3328.
- Dondurur, D. (2018). Acquisition and Processing of Marine Science Data. *Elsevier*, 1-35.
- Eddy, Taylor, "Multiscale Habitat Use and Effects of Resource Availability on California Spiny Lobster (*Panulirus interruptus*) Population" (2021). *Capstone Projects and Master's Theses*. 1117
- Ellison, A. M. (2019). Foundation species, non-trophic interactions, and the value of being common. *Isience*, 13, 254-268.
- Ellison, A.M., Bank, M.S., Clinton, B.D., Colburn, E.A., Elliott, K., Ford, D.R., Foster, D.R., Kloeppe, B.D., Knoepp, J.D., Lovett, G.M., Mohan, J., Orwig, D.A., Rodenhouse, N.L., Sobczak, W.V., Stinson, K.A., Stone, J.K., Swan, C.M., Thompson, J., Von Holle, B. and

- Webster, J.R. (2005). Loss of foundation species: consequences for the structure and dynamics of forested ecosystems. *Frontiers in Ecology and the Environment*, 9, 479–486.
- Erftemeijer, P. L., and Lewis III, R. R. R. (2006). Environmental impacts of dredging on seagrasses: a review. *Marine Pollution Bulletin*, 52(12), 1553-1572.
- Esri, 2019. ArcGIS Desktop; Release 10.7.1. Redland, CA.
- Foster, M. S. R., Riosmena-Rodriguez, R., Steller, D. L., and Woelkerling, W. J. (1997). Living rhodolith beds in the Gulf of California and their implications. Pliocene carbonates and related facies flanking the Gulf of California, Baja California, Mexico. *Geological Society of America special paper*, (318), 127-139.
- Foster, M. S. (2001). Rhodoliths: between rocks and soft places. *Journal of Phycology*, 37(5), 659-667.
- Foster, M. S., Amado Filho, G. M., Kamenos, N. A., Riosmena-Rodríguez, R. and Steller, D. L. 2013. Rhodoliths and rhodolith beds. *The Smithsonian Marine Science* 39: 143– 55
- Frederiksen, M., Krause-Jensen, D., Holmer, M., and Laursen, J. S. (2004). Spatial and temporal variation in eelgrass (*Zostera marina*) landscapes: influence of physical setting. *Aquatic Botany*, 78(2), 147-165.
- Gabara, S. S., Hamilton, S. L., Edwards, M. S., and Steller, D. L. (2018). Rhodolith structural loss decreases abundance, diversity, and stability of benthic communities at Santa Catalina Island, CA. *Marine Ecology Progress Series*, 595, 71-88.
- Garza, C. (2019). Landscape ecology in the rocky intertidal: opportunities for advancing discovery and innovation in intertidal research. *Current Landscape Ecology Reports*, 4(3), 83-90.
- Grall, J., and Glémarec, M. (1997). Using biotic indices to estimate macrobenthic community

- perturbations in the Bay of Brest. *Estuarine, Coastal and Shelf Science*, 44, 43-53.
- Hall-Spencer, J. M., Froggia, C., Atkinson, R. J. A., and Moore, P. G. (1999). The impact of Rapido trawling for scallops, *Pecten jacobaeus* (L.), on the benthos of the Gulf of Venice. *International Council for the Exploration of the Sea Journal of Marine Science*, 56(1), 111-124.
- Ivošević, B., Han, Y. G., Cho, Y., and Kwon, O. (2015). The use of conservation drones in ecology and wildlife research. *Ecology and Environment*, 38(1), 113-188.
- Johnston, D. W. (2019). Unoccupied aircraft systems in marine science and conservation. *Annual Review of Marine Science*, 11, 439-463.
- Joyce, K. E., Duce, S., Leahy, S. M., Leon, J., and Maier, S. W. (2019). Principles and practice of acquiring drone-based image data in marine environments. *Marine and Freshwater Research*, 70(7), 952-963.
- Kabiri, K., Rezai, H., and Moradi, M. (2020). A drone-based method for mapping the coral reefs in the shallow coastal waters—case study: Kish Island, Persian Gulf. *Earth Science Informatics*, 13(4), 1265-1274.
- Kamenos, N. A., Moore, P. G., and Hall-Spencer, J. M. (2004). Nursery-area function of maerl grounds for juvenile queen scallops *Aequipecten opercularis* and other invertebrates. *Marine Ecology Progress Series*, 274, 183-189.
- Kellaris, A., Gil, A., Faria, J., Amaral, R., Moreu-Badia, I., Neto, A., and Yesson, C. (2019) Using low-cost drones to monitor heterogeneous submerged seaweed habitats: a case study in the Azores. *Aquatic Conservation: Marine and Freshwater Ecosystems*, 29(11), 1909–1922. <https://doi.org/10.1002/aqc.3189>
- Koch, E. W., Barbier, E. B., Silliman, B. R., Reed, D. J., Perillo, G. M., and Hacker, S. D.,

- Wolanski, E. (2009). Non-linearity in ecosystem services: temporal and spatial variability in coastal protection. *Frontiers in Ecology and the Environment*, 7(1), 29-37.
- Landis, J. R., and Koch, G. G. (1977). The measurement of observer agreement for categorical data. *Biometrics*, 159-174.
- Lillesand, T., Kiefer, R. W., and Chipman, J. (2015). Remote sensing and image interpretation. *John Wiley & Sons*.
- Littler, M. M., and Littler, D. S. (1984). Relationships between macroalgal functional form groups and substrata stability in a subtropical rocky-intertidal system. *Journal of Experimental Marine Biology and Ecology*, 74(1), 13-34.
- Luff, A. L., Sheehan, E. V., Parry, M., and Higgs, N. D. (2019). A simple mooring modification reduces impacts on seagrass meadows. *Scientific reports*, 9(1), 20062.
- Mills, S., and McLeod, P. (2013). Global seamline networks for orthomosaic generation via local search. *ISPRS Journal of Photogrammetry and Remote Sensing*, 75, 101-111.
- Nelson, W. A. (2009). Calcified macroalgae—critical to coastal ecosystems and vulnerable to change: a review. *Marine and Freshwater Research*, 60(8), 787-801.
- Oliver, J. S., and Kvitek, R. G. (1984). Side-scan sonar records and diver observations of the gray whale (*Eschrichtius robustus*) feeding grounds. *The Biological Bulletin*, 167(1), 264-269.
- Oprandi, A., Mucerino, L., De Leo, F., Bianchi, C. N., Morri, C., Azzola, A., Benelli, F., Besio, G., Ferrari, M., and Montefalcone, M. (2020). Effects of a severe storm on seagrass meadows. *Science of the Total Environment*, 748, 141373.
- Orth, R. J., Carruthers, T. J., Dennison, W. C., Duarte, C. M., Fourqurean, J. W., Heck, K. L.,

- and Williams, S. L. (2006). A global crisis for seagrass ecosystems. *Bioscience*, 56(12), 987-996.
- Riosmena-Rodríguez, R. (2015). Natural History of Rhodolith/Maërl Beds: Their role in near-shore biodiversity and management. In *Rhodolith/Maërl beds: A global perspective* (pp. 3-26). *Springer*.
- Sacomanno, V. R., Bell, T., Pawlak, C., Stanley, C. K., Cavanaugh, K. C., Hohman, R., Klausmeyer, K.R., Cavanaugh, K., Nickels, A., Hewardine, W., Garza, C., Fleener, G. and Gleason, M. (2023). Using unoccupied aerial vehicles to map and monitor changes in emergent kelp canopy after an ecological regime shift. *Remote Sensing in Ecology and Conservation*.
- Santos, A. M. P. (2000). Fisheries oceanography using satellite and airborne remote sensing methods: a review. *Fisheries Research*, 49(1), 1-20.
- Steller, D. L., and Foster, M. S. (1995). Environmental factors influencing distribution and morphology of rhodoliths in Bahía Concepción, BCS, México. *Journal of Experimental Marine Biology and Ecology*, 194(2), 201-212.
- Steller, D. L., Riosmena-Rodríguez, R., Foster, M. S., and Roberts, C. A. (2003). Rhodolith bed diversity in the Gulf of California: the importance of rhodolith structure and consequences of disturbance. *Aquatic Conservation: Marine and Freshwater Ecosystems*, 13(S1), S5-S20.
- Steller, D. L., Riosmena-Rodríguez, R., and Foster, M. S. (2009). Living rhodolith bed ecosystems in the Gulf of California. *Atlas of Coastal Ecosystems in the Gulf of California: Past and Present*. University of Arizona Press, Tucson, AZ, 72-82.
- St-Pierre, A. P., and Gagnon, P. (2020). Kelp-bed dynamics across scales: Enhancing mapping

- capability with remote sensing and GIS. *Journal of Experimental Marine Biology and Ecology*, 522, 151246.
- Thomsen, M.S., Wernberg, T., Altieri, A., Tuya, F., Gulbransen, D., McGlathery, K.J., Holmer, M., and Silliman, B.R. (2010). Habitat cascades: the conceptual context and global relevance of facilitation cascades via habitat formation and modification. *Integrative and Comparative Biology*. 50, 158–175.
- Tompkins, P. A. (2011). *Distribution, growth, and disturbance of Catalina Island rhodoliths*. San Jose State University.
- Tompkins, P. A., and Steller, D. L. (2016). Living carbonate habitats in temperate California (USA) waters: distribution, growth, and disturbance of Santa Catalina Island rhodoliths. *Marine Ecology Progress Series*, 560, 135-145.
- Veettil, B. K., Ward, R. D., Lima, M. D. A. C., Stankovic, M., Hoai, P. N., and Quang, N. X. (2020). Opportunities for seagrass research derived from remote sensing: A review of current methods. *Ecological Indicators*, 117, 106560.
- Ventura, D., Bruno, M., Lasinio, G.J., Belluscio, A. and Ardizzone, G.,(2016). A low-cost drone based application for identifying and mapping of coastal fish nursery grounds. *Estuarine, Coastal and Shelf Science*, 171, pp.85-98.
- Ventura, D., Bonifazi, A., Gravina, M. F., Belluscio, A., and Ardizzone, G. (2018). Mapping and classification of ecologically sensitive marine habitats using unmanned aerial vehicle (UAV) imagery and object-based image analysis (OBIA). *Remote Sensing*, 10(9), 1331.
- Yang, B., Hawthorne, T. L., Hessing-Lewis, M., Duffy, E. J., Reshitnyk, L. Y., Feinman, M., and Searson, H. (2020). Developing an introductory UAV/drone mapping training program for seagrass monitoring and research. *Drones*, 4(4), 70.

Appendix I. Tables

Table 1. Drone Optimization Flights - record of each Catalina Island rhodolith bed flight by site (Isthmus and Emerald Bay) and date. Flights tested drone height (m), image overlap (%), camera angle (degrees), height, and image overlap. The presence indicates whether visible rhodolith beds were captured in orthomosaic (in part or whole).

A. Isthmus 7/20/2019

Flight #	Height (m)	Overlap (%)	Camera Angle (degrees)	Presence	# of photos
1	80	60	90	Y	86
2	80	60	90	Y	57
3	80	70	90	Y	59
4	70	80	90	Y	115
5	70	70	90	Y	74
6	60	70	90	Y	80
7	60	80	90	Y	135
8	80	80	90	N	21

B. Emerald Bay 7/21/2019

Flight	Height (m)	Overlap (%)	Camera Angle (degrees)	Presence	# of photos
1	60	80	90	N	144
2	60	80	90	N	111
3	80	80	90	N	76
4	100	80	90	N	57
5	100	80	65	N	46
6 (low battery)	100	80	65	N	28
7	100	80	65	N	54
8	80	80	90	N	130

*In this instance Agisoft Metashape was used.

C. Isthmus 01/13/2020

Flight	Height (m)	Overlap (%)	Camera Angle (degrees)	Presence	# of photos
1	70	80	90	N	54
2	70	80	90	N	60
3	60	80	90	N	66
4	60	80	90	Error	54

*In this instance Agisoft Metashape was used.

D. Emerald Bay 01/14/2020

Flight	Height (m)	Overlap (%)	Camera Angle (degrees)	Presence	# of photos
1	70	80	90	Y	55
2	60	80	90	Y	85
2b	60	80	90	Error	120
3	60	80	90	Error	120

Table 2. Drone vs Diver comparison - accuracy Matrix and kappa coefficient for image classification at each site and year. The accuracy matrix calculates error on machine learning software that will determine how well an image is classified in 0 to 100% agreeance and the kappa coefficient measures how well the classification and ground truth align in -1 to 1 agreeance (St-Pierre and Gagnon 2020; Landis and Koch 1997; and Lillesand et al. 2014).

Site/Year Image	Overall % accuracy	Kappa
Isthmus 2020	68.9	0.53
Isthmus 2021	56	0.41
Emerald Bay 2020	98.9	0.98
Emerald Bay 2021	70	0.55
Overall	73.4 (± 18.1)	0.62

Table 3A - D. Perimeter (m) and area (m²) estimates of rhodolith beds from SCUBA diver and drone surveys, and both is the overlap where sampling methods identified beds for two Santa Catalina Island rhodolith beds sampled at two time periods.

A Isthmus Cove 2020

Type	Perimeter (m)	Area (m ²)
Drone	331	2494
Diver	351	2459
Both	324	2050

B Isthmus Cove 2021

Type	Perimeter (m)	Area (m ²)
Drone	405	3873
Diver	392	3057
Both	373	2549

C Emerald Bay 2020

Type	Perimeter (m)	Area (m ²)
Drone	3278	6223
Diver	306	4790
Both	287	4472

D Emerald Bay 20201

Type	Perimeter (m)	Area (m ²)
Drone	531	8794
Diver	465	6109
Both	447	5195

Table 4. Perimeter estimates and the comparison of the percent difference between diver and drone measurements over the two time periods at the two sites with drone and SCUBA diver measurements in meters (m). Percent difference was calculated as $[(\text{diver}-\text{drone})/\text{diver}]*100$. Negative values indicate when drone surveys generated larger perimeter measurements than diver surveys

Site	Year	Drone (m)	Diver (m)	% differ diver vs drone
Isthmus	2020	331	351	5.70
Isthmus	2021	405	392	-3.31
Emerald Bay	2020	328	306	-7.18
Emerald Bay	2021	531	465	-14.20

Table 5. Area estimates and the percent difference between diver and drone estimates over two time periods at two rhodolith bed sites. Percent difference was calculated as $[(\text{diver} - \text{drone}) / \text{diver}] * 100$. Negative values indicate when drone surveys generated larger area measurements than diver surveys.

Site	Year	Drone (m ²)	Diver (m ²)	% differ diver vs drone
Isthmus	2020	2494	2459	-1.42
Isthmus	2021	3873	3057	-26.70
Emerald Bay	2020	6223	4790	-29.92
Emerald Bay	2021	8794	6109	-43.95

Table 6. Estimates of percent live cover calculations using SCUBA diver and drone survey data over two time periods in two rhodolith bed sites.

Location	Time	Drone Percent Live Cover	Diver Percent Live Cover
Isthmus	2020	76.5	62.75
Isthmus	2021	71.7	46.9
Emerald Bay	2020	75	93.25
Emerald Bay	2021	70.1	75.6

Appendix II. Figures



Figure 1. Map of known rhodolith beds around Santa Catalina Island based on historical diver surveys. Emerald Bay and Isthmus Cove, surveyed in this study, are in magenta. Image created in ArcGIS Pro. Rhodolith bed locations based on Tompkins and Steller (2016).



Figure 2. Orthomosaic constructed from a drone flight over Isthmus rhodolith bed at Santa Catalina Island, CA taken at 80 m altitude in July 2019. Yellow arrows indicate dense patches of rhodoliths within the bed. Scale bar is 25 meters.

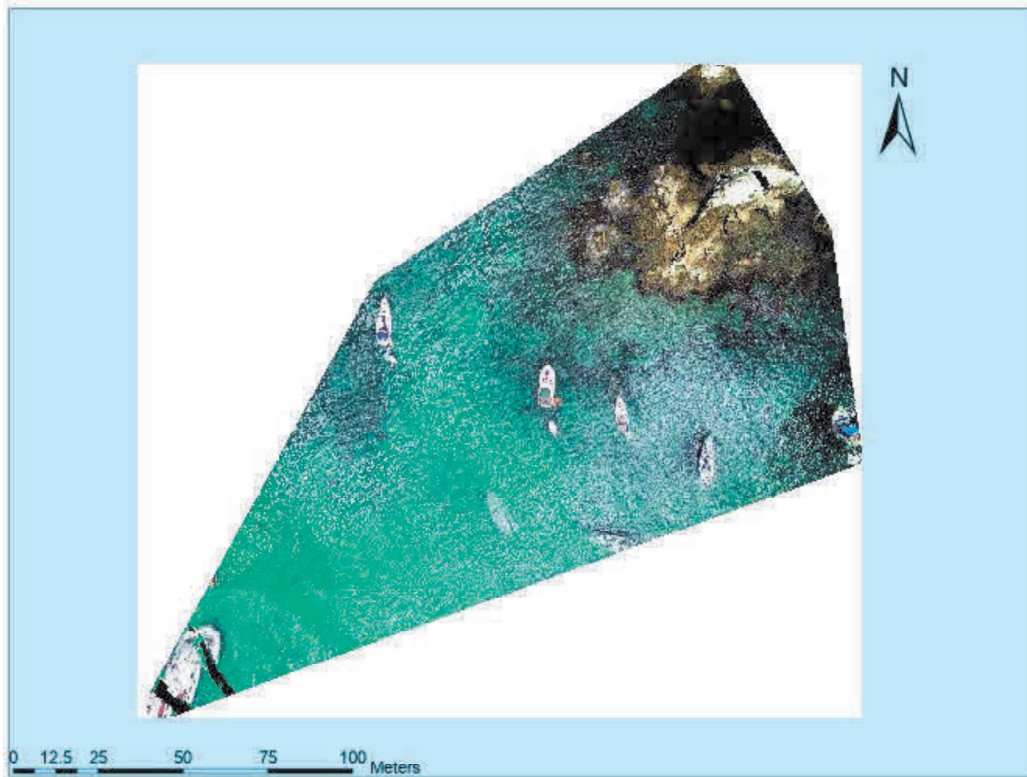


Figure 3. Orthomosaic partially constructed from a drone flight of the Emerald Bay rhodolith bed at Santa Catalina Island taken at a height of 100m, camera at 90°, 80% overlap on July 21, 2019. Glare and surface waves interfere with bed visibility.

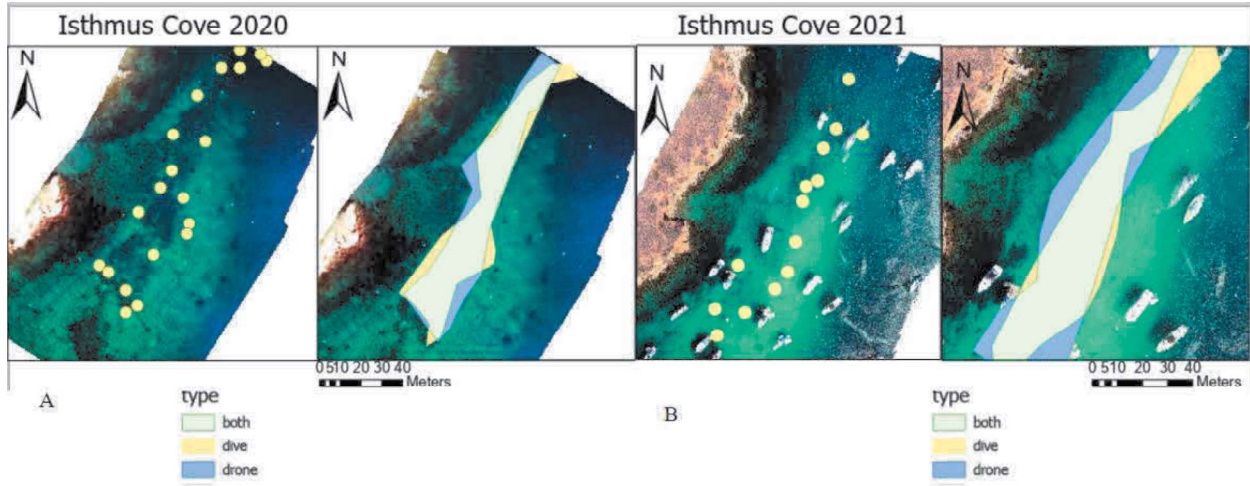


Figure 4. Orthomosaics of the Isthmus Cove rhodolith bed in January 2020 (A) and September 2021 (B). Yellow dots on the left part of the image denote the perimeter of a rhodolith bed as generated by diver-collected GPS points. On the right part of the image, an overlay depicts the area identified as rhodolith bed by diver survey only (yellow), drone survey only (blue), or detected by both (green).

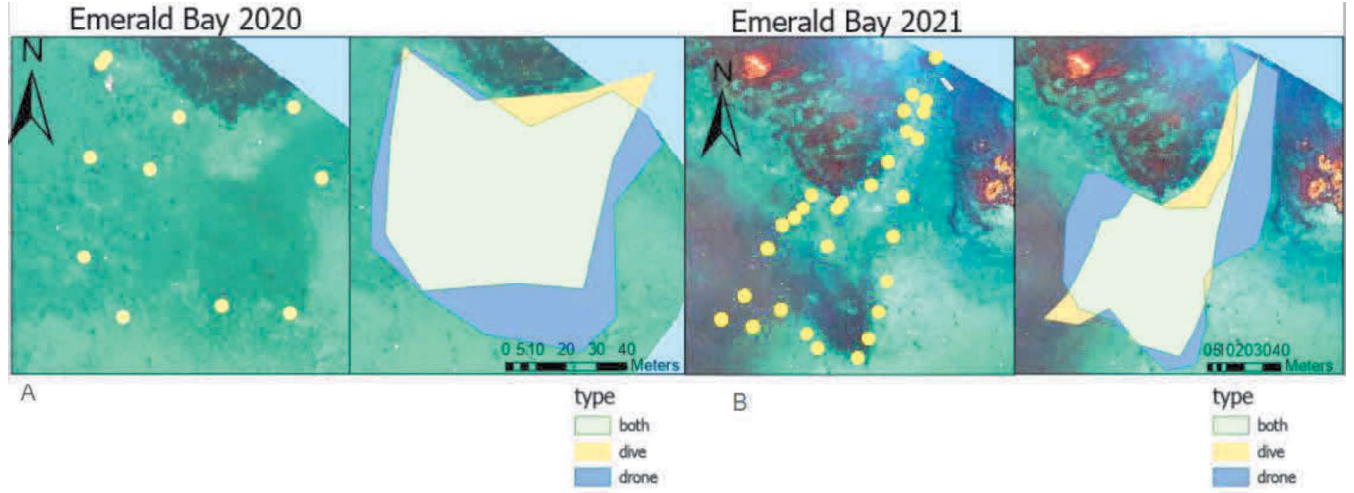


Figure 5. Orthomosaics of the Emerald Bay rhodolith bed in January 2020 (A) and September 2021 (B). Yellow dots on the left part of the image denote the perimeter of a rhodolith bed as generated by diver-collected GPS points. On the right part of the image, an overlay depicting the area identified as rhodolith bed by diver survey only (yellow), drone survey only (blue), or detected by both (green). Full extent of Emerald Bay is not depicted for 2020 and 2021 (A,B).

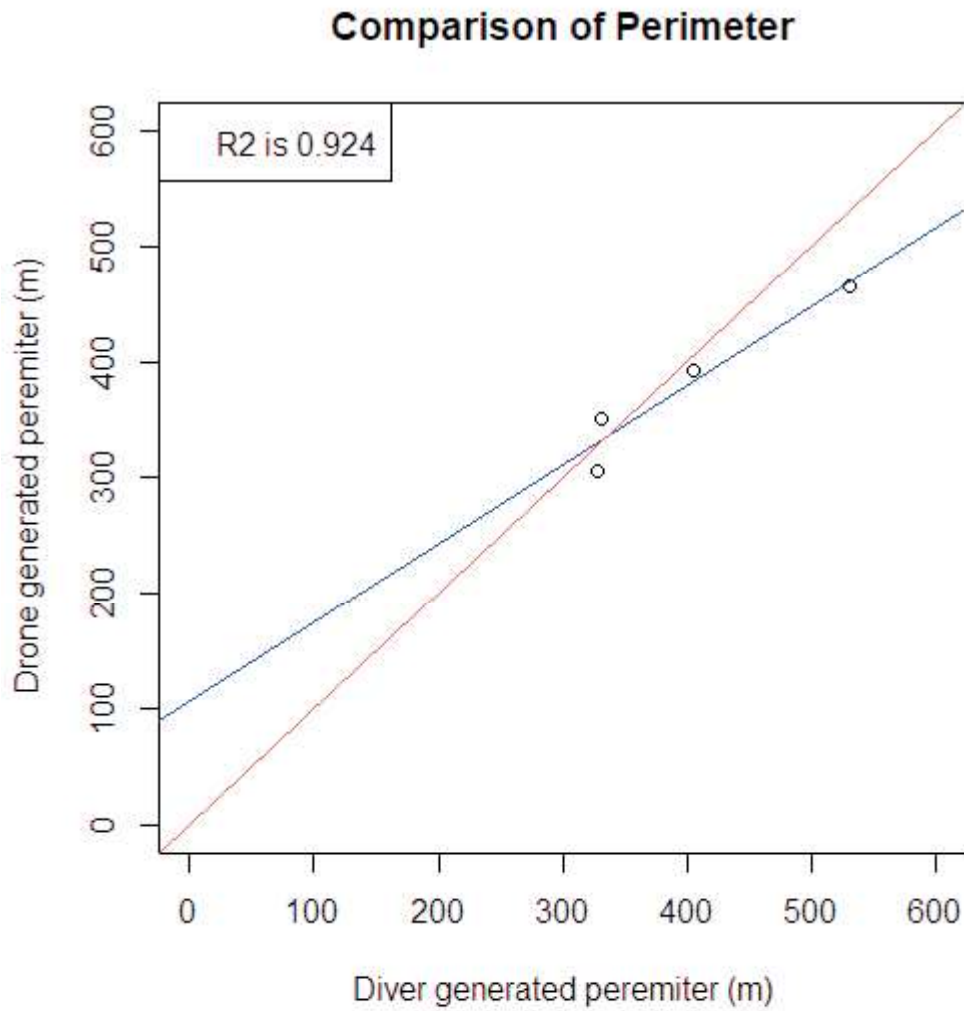


Figure 6. Relationship between diver and drone generated rhodolith bed perimeter measured at Isthmus Cove and Emerald Bay in 2020 and 2021 [$x=y$ line (red), simple linear regression $y=m(0.683)+106.579$ (blue), p -value= 0.039 and $R^2 =0.924$].

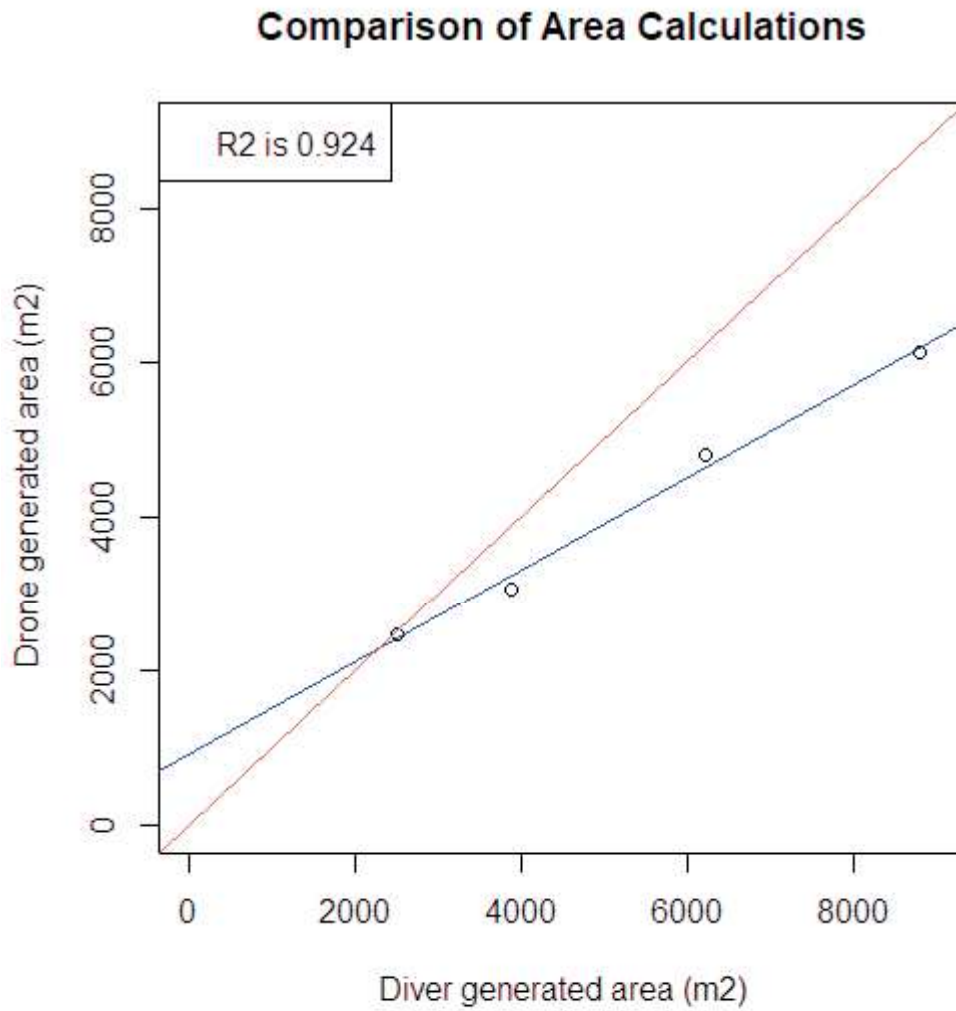


Figure 7. Relationship between diver and drone generated rhodolith bed area measurements for Isthmus Cove and Emerald Bay in 2020 and 2021 [1 to 1 line (red), simple linear regression $y=m(0.599)+902.530$ (blue), p -value= 0.004 and $R^2 =0.993$].

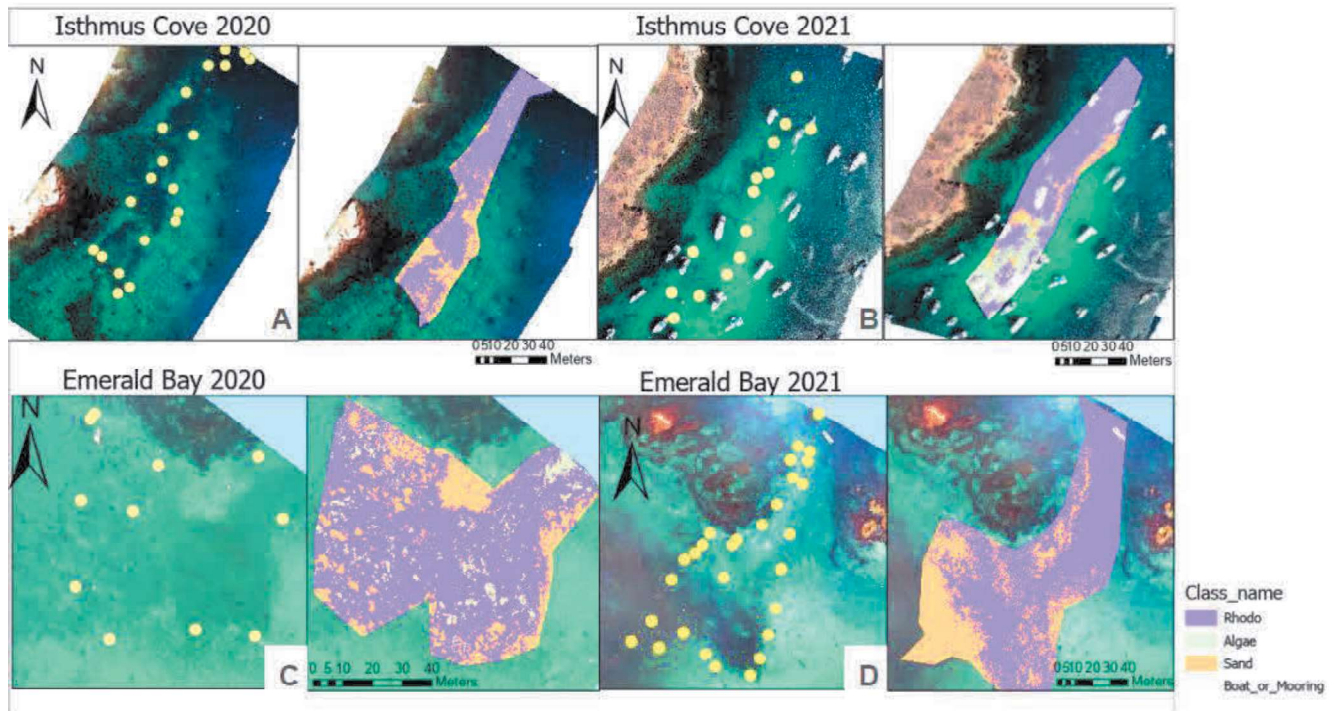


Figure 8. Side by side substrate classification images of Isthmus Cove (A, B) and Emerald Bay (C, D) rhodolith beds in 2020 (A, C) and 2021 (B, D). Left of image is the perimeter of the rhodolith bed estimated from diver-collected GPS points. On the right is the area of each rhodolith bed from the drone survey, where a maximum likelihood classification tool was used to depict dominant cover types: live rhodolith cover (pink), sand (yellow), other algae (green), and moorings and boats (white). Full extent of Emerald Bay is not depicted for 2020 and 2021 (C, D).

Extrapolation of Rhodolith Percent Live Cover

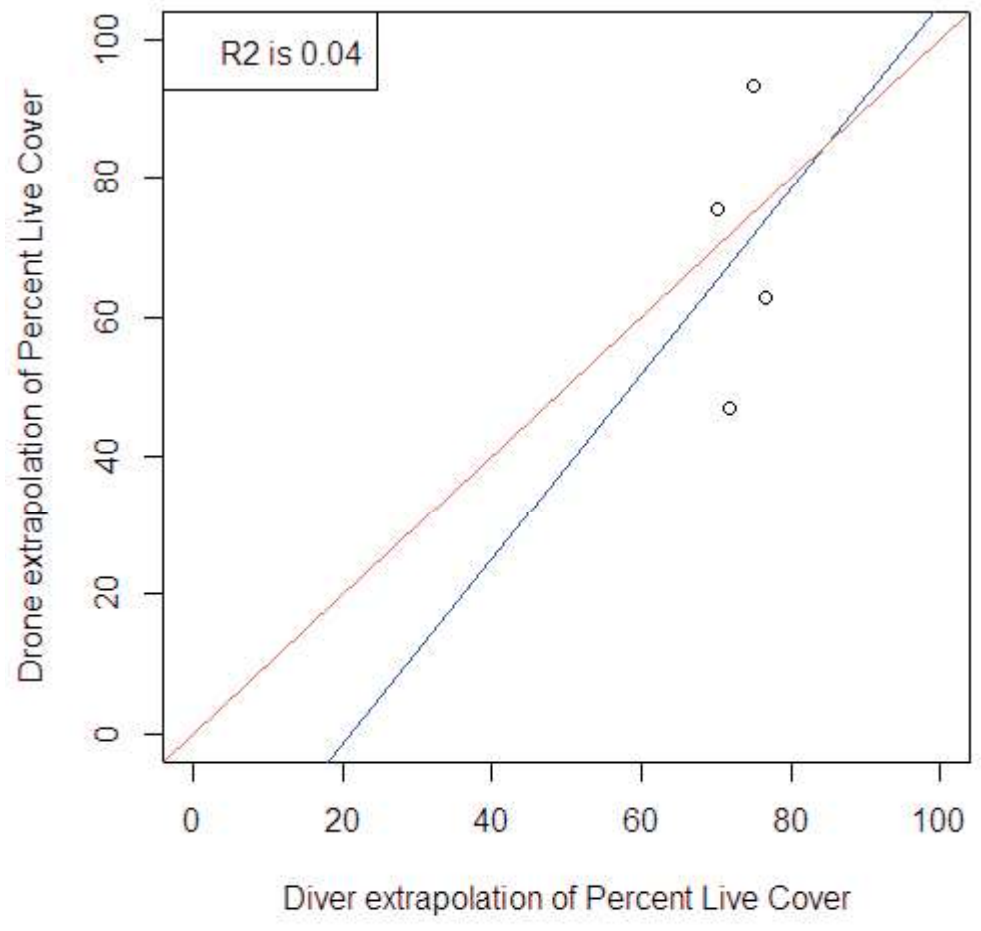


Figure 9. Relationship between diver and drone generated rhodolith bed live cover measurements for the two sites and two sampling dates [1 to 1 line (red), simple linear regression $y=m(3.115)+(-158.841)$ -blue, p-value= 0.533 and $R^2=0.218$].

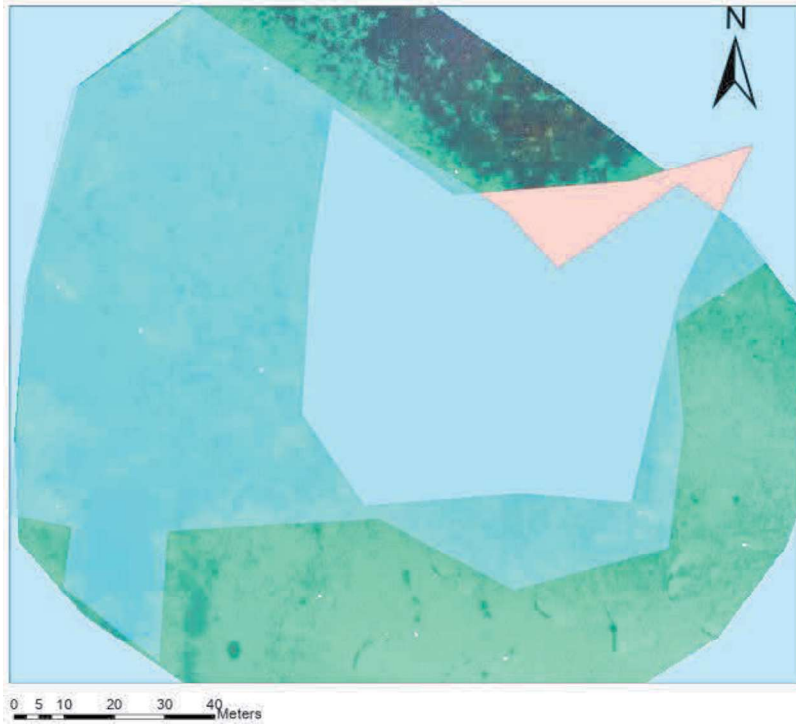


Figure 10. Overlay of drone (blue) and diver (pink) shapefiles from January 2020 sampling of the Emerald Bay rhodolith bed indicating that the drone captured more rhodolith habitat than divers could survey.

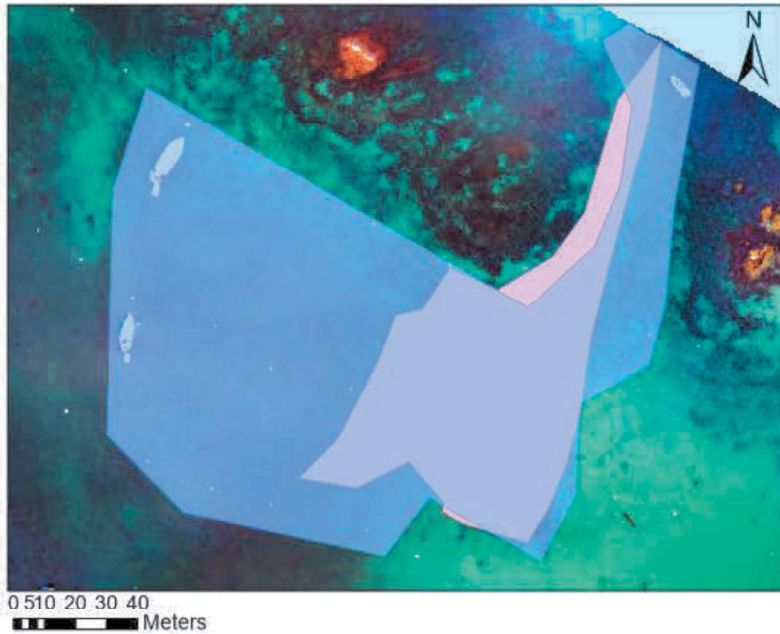


Figure 11. Overlay of drone (blue) and diver (pink) shapefiles from September 2021 sampling of the Emerald Bay rhodolith bed indicating that the drone captured more rhodolith habitat than diver could survey.

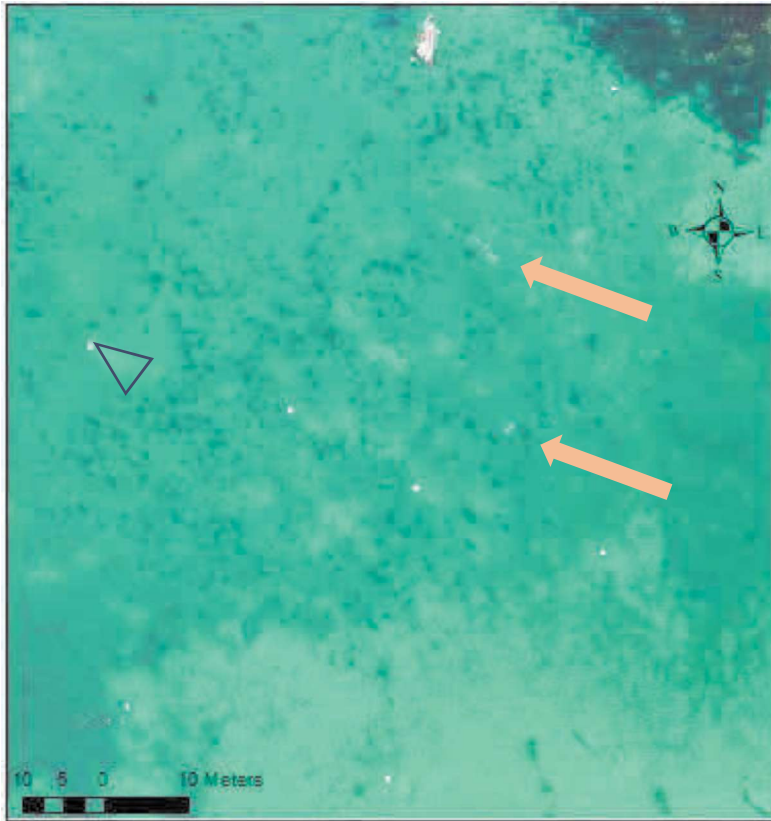


Figure 12. Evidence for drone use to identify boat mooring disturbance in rhodolith beds. Drone image of the Emerald Bay rhodolith bed showing boat mooring scars (blue triangle) and black and white 1m² markers spaced 20m apart (orange arrows). Image from drone, 80m high, January 2020.







WickliffC_SignedFinalThesis_20240510

Final Audit Report

2024-05-10

Created:	2024-05-10
By:	Amy McClintock (amcclintock@csumb.edu)
Status:	Signed
Transaction ID:	CBJCHBCAABAAwar2SLFquaaRq1nmdRwiLfQ13nw4WU31

"WickliffC_SignedFinalThesis_20240510" History

-  Document created by Amy McClintock (amcclintock@csumb.edu)
2024-05-10 - 3:22:31 PM GMT
-  Document emailed to Cindy Juntunen (cjuntunen@csumb.edu) for signature
2024-05-10 - 3:22:53 PM GMT
-  Email viewed by Cindy Juntunen (cjuntunen@csumb.edu)
2024-05-10 - 4:50:19 PM GMT
-  Cindy Juntunen (cjuntunen@csumb.edu) authenticated with Adobe Acrobat Sign.
2024-05-10 - 10:33:20 PM GMT
-  Document e-signed by Cindy Juntunen (cjuntunen@csumb.edu)
Signature Date: 2024-05-10 - 10:33:20 PM GMT - Time Source: server
-  Agreement completed.
2024-05-10 - 10:33:20 PM GMT